Chapter 5

Design, Characterization, and Environmental Applications of Hydrogels with Metal Ion Coordination Properties

Viviana Campo Dall' Orto and
Juan Manuel Lázaro-Martínez

Additional information is available at the end of the chapter

http://dx.doi.org/10.5772/62902

Abstract

In this chapter, we discuss the design and synthesis of hydrogels and related polymeric materials with metal ion coordination properties, with the aim to review the main synthetic strategies used in the area. Then, we focus on the solid-state nuclear magnetic resonance (ss-NMR) spectroscopic technique due to its importance as a structural elucidation tool in both powdered and hydrated state, with emphasis on cross-polarization magic angle spinning (CP-MAS) and high-resolution magic angle spinning (HRMAS). Also, we explain different adsorption models, with the aim to present the methods most commonly used to analyze the uptake properties of hydrogel materials toward metal ions or organic compounds. Finally, we will discuss the applications of these materials for the removal of heavy metal ions and organic compounds, in terms of efficiency in the uptake of these ions and the different techniques commonly used to study the coordination process and the generation of reactive oxygen species (ROS) from hydrogen peroxide (H_2O_2). The main aim is to provide scientists with a review of the spectroscopic techniques most commonly used for bulk and surface characterization of non-soluble materials.

Keywords: Polymers, coordination, ss-NMR, metal complexes, H_2O_2 activation

1. Introduction

Various human activities lead to increase in the concentrations of heavy metal ions in the environment. For example, the effluents from electrical and plastic industries contain copper

and cadmium ions, which are toxic and harmful, even at low concentrations, not only to humans but also to plants and animals because they are not biodegradable [1]. An effective and versatile method to remove these heavy metal ions is adsorption [2]. Thus, in the last years, many research groups have worked on the design of functionalized polymers for the development of effective and economic adsorbents for the removal of these toxics from effluents. In this context, polymeric materials with polyampholyte and polyelectrolyte characteristics have interesting properties such as acid–base behavior and coordination of inorganic and organic compounds [3]. Polymeric materials with polyampholyte characteristics consist of monomers which can have positive and negative charges, whereas those with polyelectrolyte characteristics may possess electric charge of one sign. Both can be synthesized by conventional techniques of radical polymerization [4].

Regarding the textile industry, most of the pigments used today are poorly biodegraded or resistant to environmental conditions. Thus, there is a growing need to remove these pigments from its effluents and a growing demand for new physical, chemical, and/or biological methods to reduce their concentrations [5].

With the aim to fight this pollution panorama, scientists have developed different smart systems using copper complexes of inorganic or organic material for H_2O_2 activation, thereby generating reactive oxygen species (ROS) for oxidative degradation of the pollutant. There are numerous examples of Cu(II)/organic ligand complexes as homogeneous systems in which amino acids [6], carboxylic acid [7], and Schiff bases are used as chelating agents [8], since the coordination of the metal ion produces an increase in the catalytic activity of Cu(II). In this area, heterogeneous catalysts, obtained by modifying the surface of particulate materials (such as silica, clays, and diverse polymeric materials) with Cu(II), where its efficiency is strongly dependent on the synthetic method used in their preparations, are actively being used.

In turn, the macromolecular complexes generated between ligands and transition metal ions have been widely studied because they can model the complexation of metal ions with biological ligands present in the active site of enzymes that can be emulated with carboxylic, hydroxyl, and imidazole groups present in the polymer matrix [9, 10]. Particularly, copper proteins are a group of enzymes which have copper ion as a cofactor. According to the coordination mode in the copper centers, a subclassification is carried out taking into account the geometry of the complex or the number of Cu(II) ions [11].

Nowadays, the use of biohydrogels is preferred to reduce the amount of vinyl or acryl monomers used in the preparation of synthetic hydrogels, and thus to decrease the impact on the environment. However, in general, natural materials are modified with chemical crosslinking molecules to enhance their mechanical strength and applications. Furthermore, it is interesting to obtain biomimetic Cu(II) systems that are resistant to the attack by free radicals and adverse conditions of pH and temperature, which make their recovery and reutilization possible [12–15].

http://dx.doi.org/10.5772/62902

2. Synthesis of polyelectrolyte and polyampholyte hydrogels

Ionic polymers contain covalent and ionic bonds, the latter being responsible for their acid–base and coordination properties. This class of materials is divided into two groups: polyelectrolytes, which have anionic or cationic groups, and polyampholytes, which contain both groups. For polyampholytes, the charged or ionizable groups can be located in the same or different monomer units. From the chemical point of view, polyampholytes are copolymers consisting of weak acidic and basic monomers or strong acidic and basic monomers as well as combinations of them, where the net charge and the charge distribution along the polymer chain is mainly controlled by pH changes occurring in the solution wherein the polymeric matrix is dissolved or swelled depending on the soluble behavior of the material. The net charge and the effect of the different function groups in terms of acid–base properties can be studied through potentiometric titration and the determination of the Z-potential in different conditions [16]. The first polyampholytes with weak basic and acidic groups were synthesized from acrylic acid (AA) or methacrylic acid (MAA) and 2-vinylpyridine (2VP) in the 1950s by the research group of Morawetz and Katchalsky as indicated below (AIBN: azo-bis-isobutyronitrile) (**Scheme 1**) [17]:

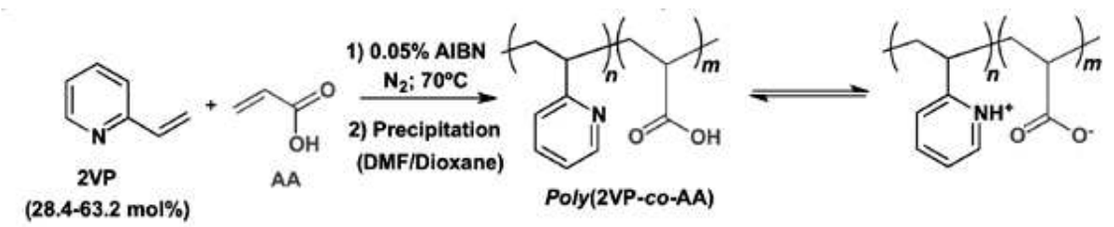

Scheme 1. Synthesis of polyampholytes materials from acrylic acid (AA) and 2-vinylpyridine (2VP).

Also, the vinyl pyridine compound can be replaced by any other vinyl basic monomers such as diethylamino-ethyl methacrylate. Using the same strategy, polymers containing sulfonic acids with vinyl or styrene residues with *N*-substituted allylamines were obtained to generate polyampholytes with strong acidic and basic groups [3]. Usually, the radical copolymerization of the acidic or basic monomers results in polymers with a statistical distribution of molecular weight due to the different reactivity of the monomers used. A classic example is the copolymerization of 2VP and MAA. The ability to ionize or to form hydrogen bonds between the monomers can greatly affect the copolymerization reaction [3].

More recently, Annenkov et al. [18] noted that the polymerization of AA or MAA with vinyl imidazole leads to a polymer contaminated with free imidazole monomers due to acid–base interactions between them [18]. This reaction leads to a deviation from the classic mechanisms of polymerization because some of the monomers are coordinated with polymer chains, decreasing the concentration of the monomers and stimulating competing reactions, such as template polymerization. Regarding this point, our research group obtained polyampholyte hydrogels from MAA, ethylene glycol diglycidyl ether (EGDE, a diepoxy compound), and imidazole (IM) or 2-methylimidazole (2MI) monomers (*poly*(EGDE-MAA-IM or 2MI)).

However, the synthetic yield was lower than that of those obtained in the synthesis of related polyelectrolyte *poly*(EGDE-MAA) and *poly*(EGDE-2MI) materials (**Scheme 2**) [16, 19].

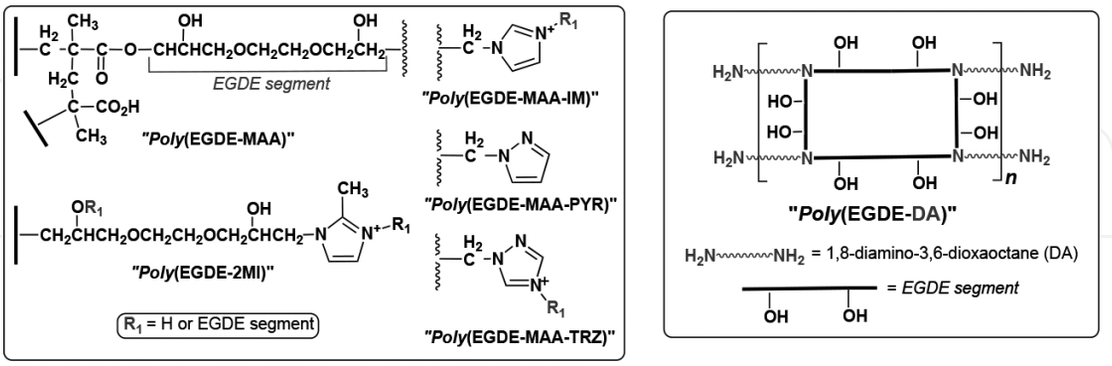

Scheme 2. Chemical structures of *poly*(EGDE-MAA), *poly*(EGDE-2MI), *poly*(EGDE-MAA-IM), *poly*(EGDE-MAA-PYR), *poly*(EGDE-MAA-TRZ), and *poly*(EGDE-DA).

Chromatographic methods led to the observation that during the evolution of the synthetic procedure of *poly*(EGDE-MAA-2MI), a new chemical compound (X) arose and remained through the synthesis with the polymer material (TLC Silica gel 60, Cl_2CH_2:CH_3OH 9:1, R_{fX}: 0.2, $R_{f\,EGDE}$: 0.8, $R_{f\,2MI}$: 0 and $R_{f\,MAA}$: 0.5). The liquid ^{1}H-NMR spectrum in Cl_3CD shows that the isolated compound, through chromatographic methods, was an ionic pair formed between 2MI (p*K*a = 7.18) and MAA (p*K*a = 4.66) monomers during the reaction. However, even when the yield of the reaction was low (45–50%) for *poly*(EGDE-MAA-IM or 2MI), it was possible to obtain functionalized polymer materials in only one simple synthetic step where IM and MAA residues were attached to a same polymer backbone with no remaining free IM molecules since all the monomers used in its synthesis were removed with acetonitrile solvent and alkaline solution during the washing step. Three parallel reactions take place in these polymer materials: radical polymerization of MAA, which gives linear segments, such as *poly*(MAA), condensation between EGDE and MAA monomers, and reaction of some epoxy units with IM, which results in N_1-substituted IM units. These N_1-substituted azole units may react with other oxirane rings to give rise to N_1,N_3-disubstituted IM units. Furthermore, linear *poly*(MAA) segments interact with azole moieties of the EGDE-IM fragments, giving some kind of interpolymeric complex, which results in an interesting system with interpenetration of linear and crosslinked polymers with application in different areas [19]. Based on this observation, our research group prepared new hydrogel materials from triazole (p*K*a = 2.39) and pyrazole (p*K*a = 2.5) molecules with a synthetic yield of around 80–90%, since these azole compounds have the advantage of not forming an ionic pair with MAA (**Scheme 2**) [16].

This evidence indicates that the best strategy to carry out the synthesis of copolymers by radical polymerization of vinyl monomers with acid–base properties is the use of the sodium salts of the corresponding acids [18]. In this way, the reproducibility of the chemical reaction is achieved, and the sodium salts of the carboxylic acids are readily obtained after precipita-

http://dx.doi.org/10.5772/62902

tion from ethanolic solutions, by the addition of equimolar amounts of sodium hydroxide. Another alternative is to carry out the synthesis of soluble polyampholytes in aqueous media using the copolymer prepared from 2-(1-imidazolyl)ethyl methacrylate (ImEMA) and tetrahydropyranyl methacrylate (THPMA), which is subsequently unprotected in the final step to generate the polyampholyte matrix as indicated below (MTS: 1-methoxy-1-trimethylsiloxy-2-methyl-1-propene, TBABB: tetrabutylammonium bibenzoate) (**Scheme 3**) [20]:

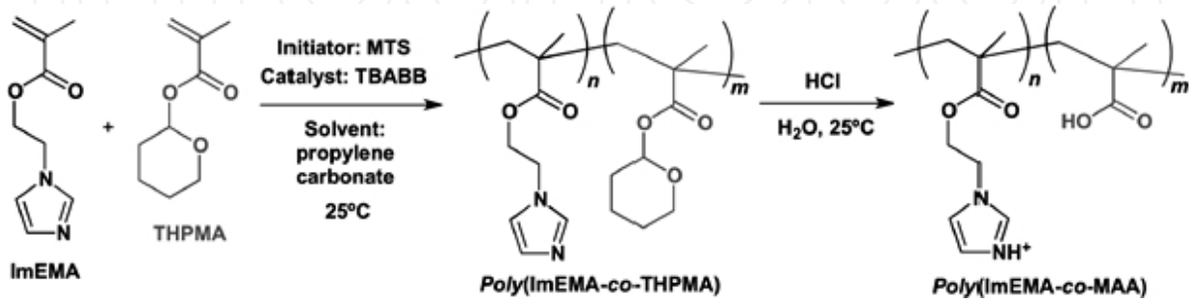

Scheme 3. Modern strategy to synthesize polyampholytes materials carrying both imidazole and carboxylic acid groups.

Significantly, these procedures require the use of monomers where the acid function is protected. The combined use of imidazole derivatives and carboxylic acids allows obtaining polymers with targeting application, such as catalysts, resins, and ion exchange matrices for solid phase extraction, which are widely applied in analytical and organic synthetic chemistry. These are materials that respond to changes in pH and ionic strength of the medium, being suitable as matrices for the uptake of inorganic and organic compounds and for controlled release of drugs and proteins [21]. Furthermore, the coordination processes may be studied during the uptake of Cu(II) ions in polyampholyte systems bearing 2-methyl-5-vinylpyridine and AA due to the catalase-like activity of the Cu(II) hydrogel toward H_2O_2 decomposition [9].

In turn, azole heterocyclic systems are interesting systems given their wide distribution in synthetic and natural compounds. In particular, our research group synthesized macromolecules containing imidazole in the structure due to the catalytic activity of this heterocyclic compound in a wide range of hydrolytic enzymes. The imidazole ring is present in most of the enzymes as part of the histidine amino acid residue, being partially responsible for catalytic activity with synergistic effect of other groups in the active site such as carboxylic acid, hydroxyl, or sulfhydryl residues. In addition, these imidazole-containing polymers have been used as anticorrosion agents [22], for protein separation [23], and as models to understand the biological activity of proteins involved in Alzheimer's disease or prion infections [24]. Furthermore, the absence of toxicity in some of these materials makes them good candidates for their use in the engineering of artificial tissues. With this purpose, Casolaro et al. synthesized polyampholytes containing methacrylate-modified L-histidine (MA-His) as outlined

below (TEA: triethylamine, EBA: *N,N*′-ethylenebis-acrylamide, and APS: ammonium peroxodisulfate) (**Scheme 4**) [25]:

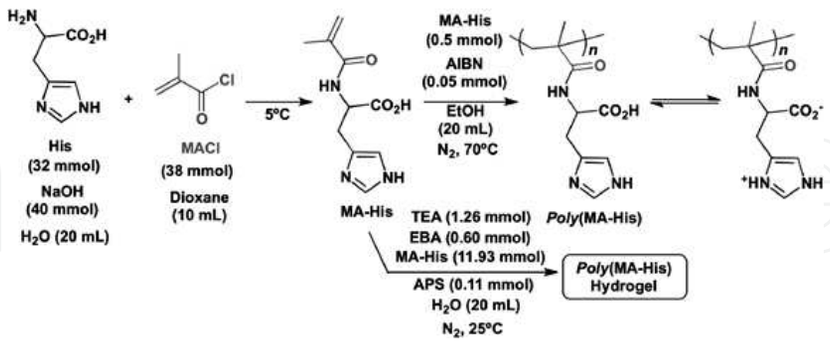

Scheme 4. Synthetic strategy for the synthesis of Poly(histidine) hydrogel materials.

The *Poly*(histidine) hydrogel is also currently being studied for its use in the controlled release of bisphosphonates to improve the bioavailability of these active drugs, together with the benefit that the polymer material is not toxic to osteoblasts [26].

Continuing the development of new polymeric materials, monomers containing epoxy groups in its structure are widely used to cause thermosetting epoxy resins, given the high degree of crosslinking that can be obtained as the curing agent used. Furthermore, the amino or carboxyl residues present in the different monomers have the chemical ability to produce the opening of epoxy groups. The reason why the imidazole molecules are highly effective for use as curing agents when added to epoxy systems is due to the fact that they can catalyze the homopolymerization of epoxide groups via a *poly*-O-etherification mechanism that leads to thermostable materials [27]. In particular, the hydrogel *poly*(EGDE-IM or 2MI) can be synthesized upon the opening of the epoxy group in the EGDE molecule by the imidazole molecules ("A") followed by a proton migration ("B"); then, an N_1-substituted imidazole unit produces the opening of another oxirane ring, allowing the *poly*-O-etherification mechanism between the alkoxide intermediate species and EGDE molecules ("C"), as indicated below for any diepoxy (DE) compound and imidazole (**Scheme 5**) [16, 27]:

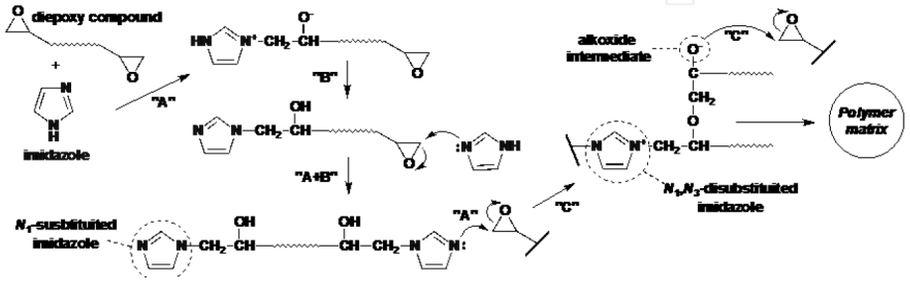

Scheme 5. Synthetic strategy for the synthesis of hydrogel materials containing imidazole groups.

http://dx.doi.org/10.5772/62902

In this way, our research group prepared an interesting polyelectrolyte hydrogel *poly*(EGDE-IM) (**Scheme 2**) bearing 55% of N_1-monosubstituted imidazole units able to be protonated or neutral, depending on the pH of the contact solution, and 45% of N_1,N_3-disubstituted imidazole units with a permanent positive charge in all the pH range, according to the measurement of the zeta potential (**Figure 1**) and potentiometric titration [16]. In contrast, the hydrogel *poly*(EGDE-MAA-IM) has a positive charge at pH values lower than 8.0 and a negative charge at pH values higher than 8.0. Thus, the polyampholyte hydrogels *poly*(EGDE-MAA-IM or 2MI) with an isoelectric point of 8.0 present a high loading capacity for bovine serum albumin (730 mg g^{-1}), together with a good desorption profile, which makes these materials acceptable for eventual applications in formulations for controlled release of proteins [19]. Even when the chemical nature of both hydrogels is quite different, the maximum loading capacity (q_m) values for copper ion uptake are around 60–70 mg g^{-1} due to the presence of the imidazole ring as the most active ligand in the coordination of the metal ion, since the *poly*(EGDE-MAA) material bearing hydroxyl and carboxyl groups takes up only 1 mg of copper per gram of polymer [10]. In the case of *poly*(EGDE-MAA), the zeta potential was zero at pH values below 4, becoming negative at pH higher than 4, as expected for a weak polyelectrolyte (**Figure 1**) [16].

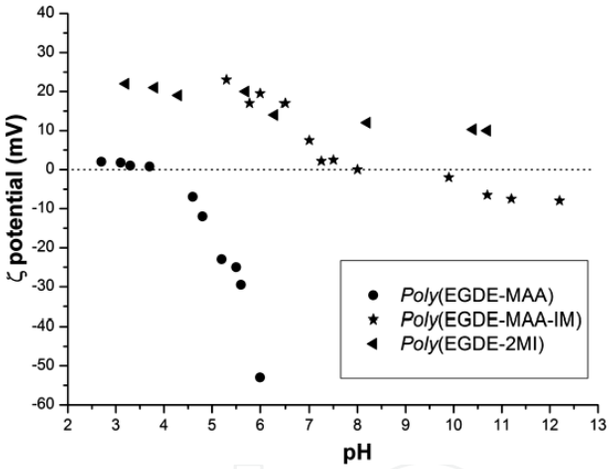

Figure 1. Effect of pH on the zeta (ζ) potential for the indicated materials [14, 16]. ζ potential measurements were performed with a zeta potential analyzer ZetaPlus from Brokhaven Instruments Corporation at 25°C and constant ionic strength of 10^{-3} M KCl. Each polymer suspension (0.25 g L^{-1}) was dispersed and shaken on a magnetic stirrer. The pH was adjusted using KOH or HCl, and the pH of the final supernatant was measured before and after the ζ potential measurements. The optical unit contains 35 mW solid-state laser red (660 nm wavelength). ζ potential was measured using a 16 V cm^{-1} electric field, 15 mA current, and 21 count times.

More traditional strategies for the design of macroporous ion exchange resins consist in the radical polymerization of glycidylmethacrylate (GMA) and ethylene glycol dimethacrylate (EGDMA) since the resulting material, *poly*(GMA-*co*-EGDMA), is versatile to be functionalized with amine groups [28]. In this sense, the group of Driessen immobilized azole ligands in *poly*(GMA-O-*co*-EGDMA) and in the sulfur derivative *poly*(GMA-S-*co*-EGDMA) after the opening of the oxirane and thiirane ring, respectively, give rise to different hydrogels with varied chemical structures (**Scheme 6**) [29]. The uptake of Cu(II) ions indicated that the

maximum loading capacities of these materials were 25 and 39 mg per gram of material for IM-SH and TRZ-SH hydrogels, respectively (**Scheme 2**). Then, the authors also synthesized similar resins by using bis-imidazole derivative compounds as a new class of azole compounds to increase the density of coordination sites. These materials showed that the uptake of Cu(II) ions was around 42 mg per gram of material, without a significant increase in the q_m compared to the above-mentioned resins containing imidazole, pyrazole, triazole, and tetrazole. However, highly Cu(II)-selective resins were obtained (**Scheme 6**) [30].

Finally, another strategy to synthesize hydrogels is the use of diepoxy (DE) with diamine (DA) compounds, which gives rise to hydrogels with high capacities for metal ion uptake. In this way, the linear chain containing --DE-DA-DE-DA-- is crosslinked by free DE molecules since the nitrogen site in the linear polymeric chain can still produce the opening of new oxirane rings [28]. In particular, *poly*(EGDE-DA) (DA = 1,8-diamino-3,6-dioxaoctane) presents a q_m for copper of 151 mg g^{-1} (**Scheme 2**) [12].

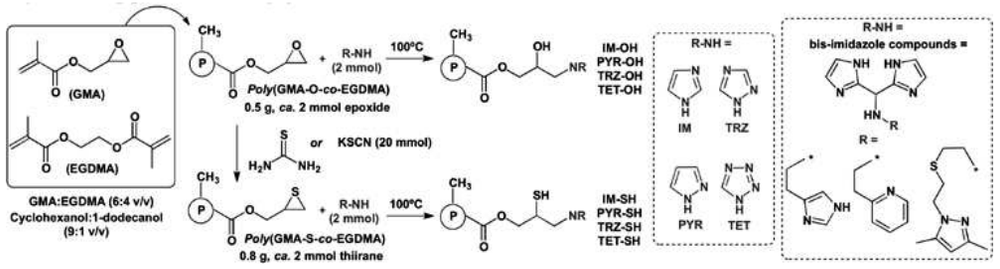

Scheme 6. Azole-modified oxirane and thiirane resins.

2.1. Natural materials

Regarding biopolymers, chitosan is one of the most widely used for the treatment of wastewater containing heavy metal ions as well as starch and cellulose. Chitosan is a *poly*(D-glucosamine) with a variable content of acetylation of the amine group since it is obtained from the deacetylation of chitin (*poly*(*N*-acetylglucosamine)). The problem that arises with the use of chitosan is that it is partially soluble in acidic solution. For that reason, to increase its chemical stability and resistance to acidic and alkaline medium as well as to increase its pore size, mechanical strength, and biocompatibility, it is chemically crosslinked with different molecules such as EGDE, glutaraldehyde, and epichlorohydrin [31]. It is important to point out that although the chemical stability is increased with the crosslinking, the q_m is reduced due to the chemical modification of the reactive sites (amino and hydroxyl groups) involved in the uptake of different metal ions. Particularly, the q_m capacity for copper ion in chitosan is 80 mg g^{-1}, whereas that for the modified chitosan with glutaraldehyde, epichlorohydrin, and EGDE is 60, 62, and 45 mg g^{-1}, respectively. Also, once these hydrogels are saturated with copper ions, they can be easily removed with EDTA solution or with acidic solution as in other Cu(II) polymer complexes and be reused many times.

Another natural polymer source to create hydrogels for the removal of pollutants together with the immobilization of enzymes is cellulose. Cellulose is a linear polymer of (1→4)-β-O-

http://dx.doi.org/10.5772/62902

glucopyranose linkage between the glucose units and with the same chemical modifications as in chitosan. Cellulose can be grafted with acrylamide or AA, increasing the partition coefficient and retention capacity of the hydrogel if the grafted cellulose is hydrolyzed. The graft polymerization of acrylamide onto cellulose presents a metal ion uptake of around 80–90% for chrome, manganese, nickel, and lead [32].

3. Characterization techniques

3.1. Nuclear magnetic resonance (NMR)

Concerning the characterization of the chemical structure of the synthesized hydrogels or any other polymeric compound, only a few spectroscopic methods, such as FT-IR, Raman, and NMR, may bring substantial chemical information. Particularly, the non-soluble behavior of these compounds prevents studying them through the common spectroscopic techniques used in the structural elucidation of soluble organic compounds. Thus, solid-state NMR (ss-NMR) experiments are used to analyze in detail the chemical structure of hydrogels and non-soluble materials in general. This technique will be briefly explained below.

Conventional liquid or solution state ^{1}H- and ^{13}C-NMR spectra are formed by narrow and well-resolved signals containing molecular information that can be interpreted by chemists. However, similar experiments performed in solid samples produce very broad signals, which can be up to several kHz or MHz, which prevents obtaining accurate information by direct observation of the spectra. This broadening also implies loss of sensitivity, especially when low-abundance nuclei such as ^{13}C (1.1%) are studied. The difference in the form of solid and liquid lines comes from the different mobility of the molecules. In the liquid state or in solution, molecules are reoriented very quickly, averaging anisotropic interactions, whereas in solid samples, this does not occur. Thus, special techniques should be applied to obtain high-resolution spectra of solids.

To resolve the structures of complex molecules, mainly chemical shifts (δ) together with the scalar coupling (J) are used. This information is obtained from NMR experiments in solution. For solid-like powder samples, these parameters are masked due to the presence of heavy anisotropic interactions such as dipole coupling and chemical shift anisotropy, which cause the widening of the signals between 0 and 50 kHz, unlike 5 kHz and 0–200 Hz for the δ and J values obtained in the liquid state, respectively [33, 34].

In fact, for spins I = ½, the Hamiltonian (H) can be expressed as follows: $\mathsf{H} = \mathsf{H}_z + \mathsf{H}_j + \mathsf{H}_d + \mathsf{H}_{cs}$, where H_z represents the Zeeman nuclear spin interaction with the applied magnetic field, H_{cs} is the chemical shift interaction arising from the magnetic fields induced by electrons, H_j is the scalar coupling interaction (J) between linked nuclei or through related chemical bonds, and H_d is the dipolar coupling interaction for each nuclear spin. In homonuclear and heteronuclear coupling, the Hamiltonians depend on the orientation of the molecule with respect to the direction of the external magnetic field. Generally, solid powder-like samples contain various crystals with random orientations where the anisotropic

interactions produce a characteristic pattern for solids since all the different molecular orientations in the sample will result in different absorption values [34]. Therefore, the information is inaccessible due to the lack of resolution of the spectrum, and it is necessary to use special techniques to increase the resolution. This is the difference with NMR in the liquid state, where the rapid movement of the molecules causes the average of the anisotropic interactions to zero to yield the isotropic chemical shift. In the solid state, the frequency of absorption for a particular crystal has spatial dependence, but all interactions have the same spatial dependence for the second term (ω) described below: $\omega \propto \frac{1}{2}(3\cos^2\theta - 1)$, where θ represents the angle between the main axis of the interaction of the tensioner and the static magnetic field B_o. This spatial dependence can be used for our convenience to obtain a high-resolution ^{13}C NMR spectrum in the solid state for example. In the 1950s, the pioneers Lowe [35] and Eades [36] showed that the widening caused by the anisotropic interactions could be averaged to zero when the sample is physically rotated about an angle θ = 54.74°. This angle was called "magic angle" (θ_m) because the spectrum obtained had narrow signals that resembled those obtained in solution. From its discovery, this technique was known as rotation at the magic angle spinning (MAS), and it is widely used in experiments in the solid state. The routine rotation speeds are between 10 and 30 kHz and up to 80–100 kHz with technological advances that have been made in this area in the last years. This is why when a sample is rotated at a spinning rate greater than the anisotropic interaction, at the magic angle, all crystals seem to have the same orientation, and the θ_m dipolar interactions are averaged to zero, reducing the width of the signals. Unfortunately, this technique is not perfect, since such widths for each signal ^{13}C resonance frequency are around 50 Hz in the solid state, but this also depends on the characteristics of the samples, being narrower when the sample is crystalline than when it is amorphous, like hydrogels.

Additionally, the sensitivity of X nuclei that exhibit low isotopic abundance, such as ^{13}C, ^{15}N, or ^{29}Si, which are typical nuclei studied through ss-NMR, can be improved by increasing the signal through the transfer of the magnetization of the abundant nuclei (^1H in general) toward the X nuclei. In solids, this technique is known as cross-polarization (CP) [37], which is optimal under certain radiofrequency field, known as the Hartmann–Hahn condition. This condition is described as follows: $\gamma_H B_1$ (^1H) = $\gamma_X B_1$(X), where γ corresponds to the gyromagnetic ratio and B_1 to the field of spin lock for each nucleus, respectively. The result of combining CP with MAS (CP-MAS) is the right strategy to obtain a high-resolution spectrum in the solid state, with adequate sensitivity for different nuclei. Therefore, it is a very valuable tool used to characterize and study insoluble materials, heterogeneous catalysts, polymorphic compounds, and pharmaceutical formulations in the solid state.

The presence of compounds containing naturally abundant nuclei, such as protons, usually generates strong interactions (either homonuclear or heteronuclear between the ^1H and ^{13}C, ^{15}N, ^{29}Si, and ^{31}P). This leads to a broadening of the signals that cannot be completely averaged, making it necessary to carry out additional techniques, including homo- and heteronuclear decoupling sequences of radiofrequency pulses to average

http://dx.doi.org/10.5772/62902

residual dipolar interactions under MAS conditions. The ^{1}H-^{13}C decoupling sequences most commonly used are SPINAL-64, Two-Pulse Phase-Modulation, and continuous-wave among others, used in the area of polymeric materials or pharmaceutical compounds [38]. In summary, the combination of MAS, CP, and heteronuclear decoupling is used for the acquisition of the ^{13}C-NMR experiment which is referred to as solid-state ^{13}C CP-MAS (**Figure 2D**).

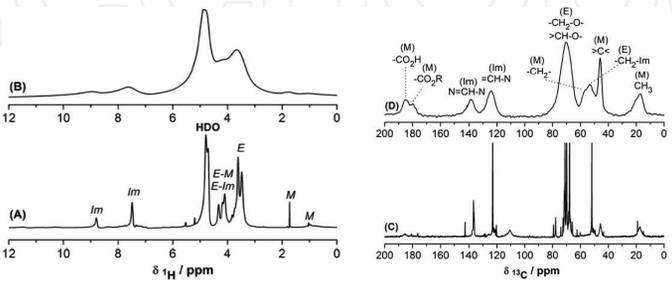

Figure 2. ^{1}H HRMAS spectra of 600 MHz for *poly*(EGDE-MAA-IM) acquired in a 4-mm HRMAS probe swelled in D_2O at a spinning rate of 4 (A) and 0 kHz or "static conditions" (B). 150 MHz ^{13}C-NMR spectrum for *poly*(EGDE-MAA-IM) acquired in a 4-mm HRMAS probe swelled in D_2O at a spinning rate of 4 kHz (C) and ^{13}C CP-MAS in a 3.2 mm ss-NMR probe at a spinning rate of 10 kHz (D). The assignment of the NMR signals corresponds to imidazole (Im), polymerized MAA (M), and EGDE (E) segments [16, 39]. All the ss-NMR experiments were performed at room temperature in a Bruker Avance III HD Ascend 600 MHz spectrometer.

In addition, the ^{13}C CP-MAS spectra can be edited to assist in the assignment of the NMR signals observed. Some of the edition techniques frequently used are the cross-polarization with polarization inversion (CPPI) [40] and non-quaternary suppression (NQS) experiments [34]. In the former, the quaternary (>C<) and methyl ($-CH_3$) carbons remain as positive signals, the methylene carbons are negative or have inverted signals, and methyne (>CH-) carbons remain in the baseline without being observed. In NQS experiments, only the quaternary and methyl carbons are visualized.

Chemists are also interested in obtaining quantitative information related to the monomer composition in copolymer materials or in any modification made in the polymer structure. However, this information is difficult to obtain because it is necessary to apply ^{13}C direct polarization techniques (^{13}C DP), which require the use of the NMR spectrometer for a long time, and because not all the polymeric powders give rise to an adequate signal-to-noise ratio. In contrast, ^{13}C DP spectra can be very useful to provide quantitative information related to the crystalline and amorphous amounts in crystalline or semicrystalline polymers. For instance, our research group studied semicrystalline *poly*(ethylenimine) hydrochloride systems ($[-CH_2-CH_2-NH(HCl)-]_n$) due to the different environments of the crystalline and amorphous domains where the polymeric segments in the crystal lattice are confined. We observed two well-resolved ^{13}C resonance signals at 44.5 and 42.9 ppm, being the signals associated with the amorphous and crystalline regions, respectively [41].

Regarding ^{1}H-NMR spectra, it is necessary to point out that these kinds of simple experiments are not determined as routine in the solid state because the dipolar coupling among protons is higher than the commonly spinning speed obtained by the commercial NMR probes (10–35 kHz). However, partially or well-resolved ^{1}H spectra can be obtained at high spinning rate (>60 kHz) or with particularly high-power decoupling techniques at moderate spinning rate. In general, proton spectra of solid polymer samples consist in wide lines and in some cases an overlapping of wide and sharp lines at static conditions [34].

Fortunately, for hydrogels, there is an experiment called high-resolution magic angle spinning (HRMAS), where the ^{1}H-^{1}H dipolar interactions can be partially averaged, rendering liquid-like ^{1}H-NMR spectra similar to those observed for liquids. In this technique, the material is swelled with deuterated solvents, making it possible to expand the analysis of hydrogel compounds and tissue samples [42, 43]. Another advantage of this technique is that the sample is not spun at high rates because at 2–4 kHz the residual ^{1}H–^{1}H dipolar couplings, which were partially averaged by the swelling produced by the solvent, are eliminated (**Figure 2**). The deuterated solvents that can be used are the same as in the liquid state since the HRMAS probe is designed with a deuterium channel (^{2}H) to lock the NMR signal. The sample is placed in special zirconia rotors with different volumes as in ss-NMR, with the difference that they are designed with cylindrical spacers to contain the sample. In this way, HRMAS experiments allow chemists to study hydrogels or swelled samples as in liquid-state NMR (**Figure 2A** and **B**).

Although all these examples are very interesting, the ss-NMR technique has to achieve some sensitivity limits that make this spectroscopic tool not able to analyze small chemical modifications of materials or encapsulation of molecules among others. However, these sensitivity problems can be partially resolved with the use of dynamic nuclear polarization (DNP) experiments for solid samples [44–46]. In this technique, the powder sample is impregnated with a biradical solution and introduced in a zirconia rotor which will be spun at the magic angle at ~90–100 K. At this temperature, the polarization transfer is increased from the electron of the radical molecules to the proton network of the material under study, allowing the polarization of the spins in the material under study through spin diffusion. To polarize the electron of the radical molecules, microwave irradiation is on throughout the experiment. For protons, the maximum theoretical enhancement achievable is given by the gyromagnetic ratios (γ_{e-}/γ_{1H}), being around 660.

3.2. X-ray photoelectron spectroscopy (XPS)

Several spectroscopic analyses exist for surface characterization, but the most commonly used to conduct this experiment is based on the irradiation of the surface of the sample with monochromatic X radiation, called X-ray photoelectron spectroscopy (XPS), also known as electron spectroscopy for chemical analysis (ESCA) [47]. This spectroscopic technique allows identifying all the elements of the periodic table, except hydrogen and helium, but more importantly it allows determining the oxidation state of an element and species to which it is attached, thus providing valuable information on the electronic structure of the molecules.

http://dx.doi.org/10.5772/62902

Due to the short penetration power of the electrons, this technique only provides information on a surface layer of a thickness of 20–50 Å. The most important and valuable application of XPS is for the qualitative analysis of the surfaces of solids, such as metals, alloys, polymers, semiconductors, and heterogeneous catalysts. It also allows quantifying each element on the surface, having into account their sensitivity factors.

XPS records the kinetic energy of the emitted electrons after a monochromatic X-ray beam of known energy (hv) affects the surface of the testing sample. This causes the release of an electron from a K orbital with specific energy E_b. The reaction can be represented as follows: $A + hv \rightarrow A^{+*} + e^{-}$, where A can be an atom, a molecule or an ion, and A^{+*} is an electronically excited positively charged ion. The kinetic energy (E_k) of the emitted electron is measured in the electron spectrometer. In this way, the electron binding energy (E_b) can be calculated by the following equation: $E_b = hv - E_k - w$. In this equation, w is called the work function of the spectrometer, a correction factor of the electrostatic environment in which the electron is formed and recorded. The value of w can be determined by several methods. The E_b is characteristic of an electron orbital of the atom, wherein the electron was released.

As a result, an XPS spectrum is a graph of the number of emitted electrons (or electron beam power) based on E_b. The high background level observed occurs because with each characteristic peak there is a queue due to the ejected electrons that have lost some of their energy in inelastic collisions inside the solid sample. These electrons have less kinetic energy than equivalent non-dispersed electrons and therefore appear at higher binding energies.

Simultaneously, Auger electron emissions are originated throughout the interaction with X-ray. The Auger process emissions are generated during the relaxation of the excited ion A^{+*} after interacting with a beam of monochromatic X-ray photons, where an Auger electron is emitted at the same time as an ion A^{++} is generated on the surface of the material under study. These emissions are described according to the type of orbital transitions involved in the production of the electron (KLL, LMM, or MNN Auger transitions). The applications of XPS in hydrogels and copper–hydrogel complexes will be discussed in the last part of this chapter.

3.3. Other characterization techniques

Another technique for the study of heterogeneous catalysts or hydrogel-containing paramagnetic centers is electron paramagnetic resonance (EPR), also called electronic spin resonance (ESR). This technique is based on the absorption of electromagnetic radiation in the microwave region of a sample with paramagnetic electronic properties which is subjected to a magnetic field. However, this magnetic field is not as intense as in NMR. EPR allows obtaining information about the different geometries adopted by paramagnetic ions when they are part of either biological complexes or biomimetic systems, as well as of heterogeneous catalysts [10, 11]. An important difference with any other spectroscopic technique is that in the EPR spectra, the first derivative absorption line is plotted. The number and intensity of the EPR lines depend on the interaction between the unpaired electron spin (S = 1/2) and the nuclear spin (I, i.e. I_{Cu} = 3/2). The application and examples of EPR experiments will be discussed later in this chapter.

Other complementary techniques for the study of surfaces include the following:

- Scanning electron microscopy (SEM) and atomic force microscopy (AFM), which can provide information on the physical microstructure by images of morphology and topography.
- Energy dispersive X-ray diffraction (EXD) experiments, which allow obtaining a semiquantitative elemental composition of the surface of the material observed by SEM microscopy and analyzing the distribution of a particular element such as spreading of a metal ion in a particular section of interest.
- N_2 adsorption isotherms, which allow measuring the specific surface area by using the nitrogen adsorption isotherm BET [48]. The advantage of this approach is that it allows estimating the surface area and pore dimensions of different materials together with the interior texture of particles.

4. Metal ion uptake equilibria and characterization techniques

To analyze the sorption processes involved in the uptake of different inorganic (metal ions) or organic compounds (dyes, proteins, pollutants, among others), different models can be used, and these will be discussed in this section.

When a gas or solute in a solution affects a solid surface, it can either bounce or remain attached (*adsorbed*). The sorbate can diffuse on the surface, remain attached, undergo a chemical reaction, or be dissolved in the solid (this last process is known as *absorption*). Two different behaviors can be distinguished: physisorption and chemisorption, although intermediate situations are often found.

In physisorption, the molecules remain attached to the surface of the sorbent by means of van der Waals forces (dipolar interactions, dispersion, and/or induction). In chemisorption, the molecules remain attached to the surface, forming a strong covalent binding, and the chemisorption enthalpies are higher than the physisorption enthalpies and are generally exothermic processes that stop after monolayer formation on the surface. Chemisorption involves the breakdown and formation of bonds. This is why the chemisorbed molecule does not preserve the same electronic structure as in the former phase.

The equilibrium of metal ion uptake can be explored by analyzing the results of the adsorption isotherm for the polymeric adsorbent at a given temperature. Several isotherm models are generally used to fit the experimental data of the adsorption of ions or any other molecule on particles by nonlinear regression. These models include the Langmuir adsorption isotherm, the Freundlich equation, the Temkin model, and the Dubinin–Radushkevich isotherm, each of which is described below.

The Langmuir adsorption isotherm is derived from theoretical models, provides information on uptake capabilities, and reflects the usual equilibrium process behavior but does not provide information about the mechanistic aspects of adsorption. The equation is $q_e = \frac{q_m C_e}{K_L + C_e}$,

http://dx.doi.org/10.5772/62902

where q_e is the adsorption capacity in equilibrium with the corresponding C_e (M), which is the concentration of metal ion, q_m is the maximum adsorption capacity, and K_L is the equilibrium constant of dissociation. In some cases, the linear form is preferred to simplify the analysis of the experimental data [31]. The Langmuir equation assumes a homogeneous surface of the adsorbent (a flat surface), a single site per molecule (monolayer), and no interaction between the adsorbed species and adjacent active sites [49]. The change in free energy related to the ion uptake can be calculated from: $\Delta G = -R\ T\ \ln K_a$, where R (8.314 x 10^{-3} kJ mol^{-1} K^{-1}) is the gas constant, T is the thermodynamic temperature, and K_a (M^{-1}) is the equilibrium constant of association ($1/K_L$). The negative sign of this thermodynamic parameter indicates the spontaneous nature of the reaction.

The Freundlich equation is described as $q_e = K_F\left(C_e^{\frac{1}{n}}\right)$. This model assumes that the surface is heterogeneous in the sense that the adsorption energy is distributed, and the surface topography is patchwise [50]. The sites with the same adsorption energy are grouped together into one patch (the adsorption energy here is the energy of interaction between the adsorbate and the adsorbent). Each patch is independent of each other (i.e., there is no interaction between patches), and the Langmuir equation is applicable for the description of equilibrium of each patch. In fact, this isotherm can be theoretically derived supposing that the surface has different types of adsorption sites. K_F can be defined as the sorption or distribution coefficient and represents the amount of sorbed molecules/ions onto the polymer surface normalized by the equilibrium concentration and $1/n$ is a measure of surface heterogeneity. When the value of n becomes larger than about 10, the adsorption isotherm approaches a so-called irreversible isotherm, because the concentration needs to go down to an extremely low value before the adsorbate molecules desorb from the surface [50].

The Temkin model is empirically derived and assumes that the heat of adsorption (which is a function of temperature) of all molecules in the layer will decrease linearly rather than logarithmically with coverage [51]. It allows estimating the equilibrium constant and the adsorption heat: $q_e = \frac{R\ T}{b_T}\ln(K_T C_e)$.

The Dubinin–Radushkevich isotherm is a semi-empirical equation which was originally developed for subcritical vapors in microporous solids, where the adsorption process follows a pore-filling mechanism: $q_e = q_m e^{-B_D \epsilon^2}$, where q_m is the maximum amount of adsorbate that can be adsorbed in micropores, and B_D is a constant related to the energy.

Liquid-phase adsorption data can also be analyzed by the equation below, where the amount adsorbed corresponding to any adsorbate concentration is assumed to be a Gaussian function of the Polanyi potential (ε): $\epsilon = R\ T\ \ln\left(1 + \frac{1}{C_e}\right)$, where C_e represents the solute concentration at equilibrium (g solute per gram of solution) [52]. This equation is generally applied to express the adsorption mechanism with a Gaussian energy distribution onto a heterogeneous surface. The approach is usually applied to distinguish the physical and chemical adsorption of metal ions by means of the equation $E = \frac{1}{\sqrt{2B_D}}$. The parameter E is the mean free energy of sorption [53], whose magnitude is a way to estimate the type of sorption process. In

the case that E is lower than 8 kJ mol^{-1}, weak physical forces, such as van der Waals and hydrogen bonding, may affect the sorption mechanism. If this value is between 8 and 16 kJ mol^{-1}, the sorption process can be explained by ion exchange. If this value is higher than 16 kJ mol^{-1}, the sorption process can be explained by other chemical reactions such as coordination [54].

The isotherm parameter sets with statistical support can be determined by nonlinear regression, using the algorithm based on the Gauss–Newton method. An error function can be used to evaluate the fit, the second-order corrected Akaike information criterion (AIC):

$$AIC = N \ln\left(\frac{RSS}{N}\right) + 2P$$

$$AIC_c = AIC + \frac{2P(P+1)}{N-P-1}$$

where P is the number of parameters in the model, N the number of data points, and RSS the residual sum of squares [55]. Δ AIC represents the difference in AIC values between two competing models. The associated Akaike weights for the better and worse models are:

$$W_{better} = \frac{1}{1+e^{-\frac{1}{2}\Delta AIC}}$$

$$W_{worse} = \frac{e^{-\frac{1}{2}\Delta AIC}}{1+e^{-\frac{1}{2}\Delta AIC}}$$

The Akaike weights provide information about the strengths of evidence supporting the two competing models. The ratio of the two Akaike weights, W_{better}/W_{worse}, is termed as the evidence ratio and represents the relative likelihood favoring the better of two competing models. As reported by other authors, an evidence ratio greater than 20 would indicate extremely strong evidence favoring the better model [56]. Another fundamental aspect of the uptake of metal ions or organic molecules for industrial application is the knowledge of the kinetic parameters ruling this process and the rate-controlling step of the sorption process. For this reason, the adsorption capacity of the adsorbent is usually studied as a function of time. The sorption mechanism could be controlled either by a chemical reaction or by diffusion processes, such as pore and film diffusion. If the experiments are performed in a well-stirred batch system, the thickness of the boundary layer surrounding the particle should be minimal, and boundary layer resistance or film diffusion should not be major rate-controlling factors [57]. Besides, the particles can have mesopores and macropores, expected to be accessible for different metal ions and small organic molecules in general. If the contact time necessary to achieve equilibrium conditions is short, it might initially indicate that the adsorption of the studied cations

http://dx.doi.org/10.5772/62902

is a chemical-reaction-controlled process [58–60]. For example, the *poly*(EGDE-MAA-2MI) hydrogel with polyampholyte properties (**Scheme 1**) was tested as adsorbent for the removal of Pb(II) and Cd(II) from aqueous solutions. The metal ion uptake equilibration end point could be estimated in 10 hours for Cd(II), even if the 80% of the load was reached in less than 3 hours. For Pb(II), the equilibrium was reached in a shorter time. These results evidenced a chemical-reaction-controlled process. In this case, a network expansion was predicted as a result of repulsive interaction between the fixed positive charges. The same kinetics profile was found for Cu(II) and Co(II) ions, with this type of adsorbents [61].

Different kinetic models can be used to fit the experimental adsorption data by nonlinear regression. The Elovich equation is based on a general second-order reaction mechanism for heterogeneous chemisorption processes and is formulated as: $\frac{d\,q_t}{dt} = \alpha e^{-\beta q_t}$, where q_t is the amount of adsorbed ion at the contact time t [57, 58]. After integration and application of the boundary conditions, for q_t = 0 at t = 0 and q_t = q_t at t = t, the equation becomes [57] $q_t = \frac{1}{\beta}\ln(1 + (\alpha\ \beta\ t))$. Teng and Hsieh proposed that constant α is the initial adsorption rate, and β is related to the extent of surface coverage and the activation energy involved in chemisorption [62]. This equation assumes that the active sites of the sorbent are heterogeneous in nature and therefore exhibit different activation energies for chemisorption [57]. Another explanation for this form of kinetic law involves a variation of the energetics of chemisorption with the extent of surface coverage [62].

The modified Freundlich model was originally developed by Kuo and Lotse: $q_t = k_F C_o\left(t^{1/m}\right)$, where k_F is the apparent adsorption rate constant, C_o is the initial ion concentration, and m is the Kuo–Lotse constant [63]. Bache and Williams indicated that the energy of adsorption decreases exponentially with increasing surface saturation when the adsorption fits the Freundlich equation. Everett suggested an increase in the perturbation potential as a consequence of the interactions between the species at close distance [64]. In concordance with this theory, k_F usually decreases as C_o increases. This modified Freundlich model can describe a surface-diffusion-controlled process different from intraparticle diffusion. Instead, when the estimated m parameter is close to 2, the kinetics is controlled by the intraparticle diffusion in the pores, involving the movement of the adsorbing ion along the walls of the less accessible spaces of the adsorbent and the diffusion into the solid itself.

In addition, most metal ion sorption system models in the literature are based on reaction kinetics using pseudo first-order kinetics or pseudo second-order kinetics. The pseudo first-order model suggests that one ion sorbs to one active site. The integrated equation by applying the boundary conditions, for q_t = 0 at t = 0 and $q_t = q_t$ at $t = t$, is $q_t = q_e\left(1 - e^{-kt}\right)$, where q_e is the amount of cadmium sorbed at equilibrium as well as the equilibrium adsorption capacity of the sorbent, and k is the rate constant. A series of pseudo first-order terms involves different types of binding sites, and in each case, the stoichiometric ratio between the binding site and the adsorbate molecule or ion is 1:1. The pseudo second-order model is described by

$$q_t = \frac{q_e^2 k\ t}{1 + (q_e k\ t)}$$

$$h = q_e^2 k,$$

where k is the rate constant of the pseudo second-order equation, and h is the initial adsorption rate. The pseudo second-order kinetic model presupposes that each metal ion binds to the active sites on the surface in a 1:2 stoichiometric ratio [57, 65]. The experimental kinetic results of Cd(II) and Pb(II) uptake on *poly*(EGDE-MAA-2MI) hydrogel fitted different models, depending on the initial metal ion concentration. For lower concentration levels, the best model was the modified Freundlich. At higher concentration values, Cd(II) uptake followed the Elovich model, and Pb(II) the pseudo first-order model with two parameters. It could be concluded that the kinetic models that better fitted these results were those that described variations of the energetics of chemisorption with the extent of coverage due to interactions between the involved species [61].

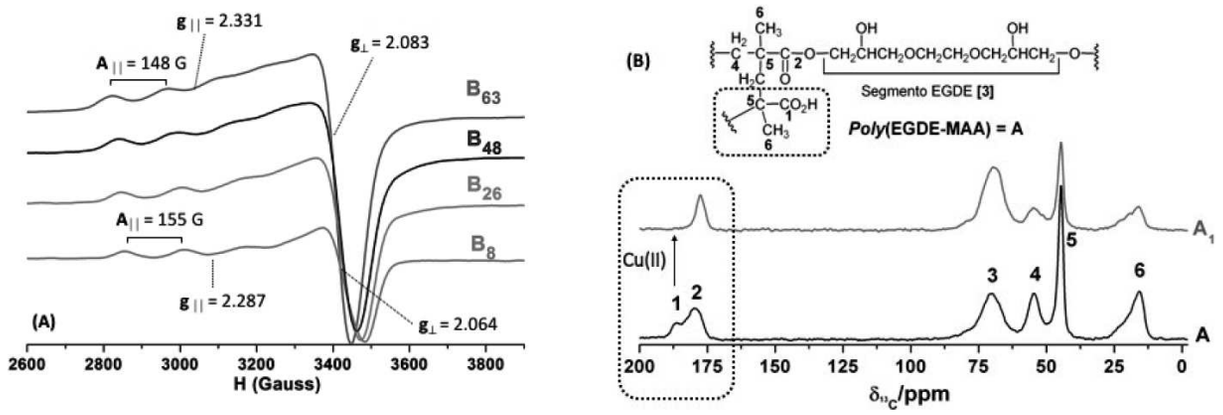

Figure 3. X-band EPR spectra for the solid Cu(II) *poly*(EGDE-MAA-IM) complex (**Scheme 1**) with different copper ion content (*B*x = x mg copper per gram of complex as determined from the direct measurement of the solids through X-ray fluorescence (XRF) in an advant XP+ thermo electron spectrometer) (A) [10]. ^{13}C CP-MAS for *poly*(EGDE-MAA) and its Cu(II)-complex (**Scheme 1**) with 1 mg Cu(II) g^{-1} = A_1 (B) [66]. EPR measurements of the Cu(II)-complexes were performed at X-band on a Bruker EMX plus spectrometer at 20°C. The ss-NMR experiments were performed at room temperature in a Bruker Avance-II 300 MHz spectrometer. The different Cu(II) complexes were obtained from the adsorption of Cu^{2+} ions on the different polymers by batch adsorption experiments. Each material (0.1000 g) was placed in contact with 2 mL of cupric sulfate ($CuSO_4$) solution in a 4–100 mM concentration range. The resulting suspensions were shaken in a thermostatic bath at 25°C for 24 hours. Then, the samples were centrifuged, filtered, and dried at 60°C for 24 hours.

Although all these analyses allow the complete characterization in terms of physicochemical aspects, they do not allow obtaining information related to example with the ligands involved in the uptake of metal ions. For that reason, complementing them with spectroscopic techniques can bring important information related to chemical aspects associated with the

http://dx.doi.org/10.5772/62902

coordination process in different conditions. Our research group, for example, studied the coordination sphere of copper ions in the synthetic Cu(II) hydrogel complexes by using a combination of ss-NMR and EPR techniques [10, 66]. The EPR spectra of isolated Cu(II) centers with a minimum distance of 10–15 Å between each paramagnetic nucleus provide more information because the values of parallel hyperfine coupling constant ($A_{||}$) and parallel *g*-factor ($g_{||}$) obtained from the hyperfine structure of the Cu(II) complexes differ depending on the geometry and the ligands of the paramagnetic entity (**Figure 3A**). In general, the EPR parameters show that when oxygen becomes more active in the uptake of copper ions, the $A_{||}$ values decrease, and the $g_{||}$ values increase as the amount of ions in the polymeric structure increases. However, EPR spectroscopy must be used together with ss-NMR or any other spectroscopic technique due to the broad range of materials and chemical compositions, because the elucidation of the chemical sphere of Cu(II) centers based on EPR does not result in a clear-cut result [10]. For Cu(II) proteins and any other Cu(II) materials, the Peisach–Blumberg plots can be very useful to access to the coordination sphere of the paramagnetic center [10, 67]. On the other hand, the ss-NMR technique retrieves information of the ligands involved in the coordination of paramagnetic ions due to the enhancement in the relaxation behavior of the different nuclei present in the polymer matrix (^{1}H, ^{13}C, ^{15}N, etc.), avoiding the detection of resonance signals. In particular, ^{13}C CP-MAS experiments are effective to study the preferences in the uptake of Cu(II) ions at different concentrations of the metal ions in polyelectrolyte and polyampholyte materials. However, some experimental conditions, such as the contact time used in the cross-polarization step in ^{13}C CP-MAS experiments, must be taken into account before setting the acquisition parameters. For example, for a Cu(II) hydrogel (*poly*(EGDE-MAA-IM)) bearing carboxylic acid as ligand for copper ion, it is possible to observe how the signal corresponding to the carbon of these groups is affected after the uptake of the paramagnetic ion and is thus not detected (**Figure 3B**) [10, 66]. This strategy to study the coordination of copper ions can also be used to understand the uptake of zinc [68], mercury [69], cobalt [13], and samarium [70] ions in polymer matrixes.

The uptake of Cu(II) ions allows that different ligands distributed in the same or different polymeric chains of the adsorbent material participate in the coordination process, modifying the polymer properties. Particularly, the glass transition temperatures (T_g) are increased as a consequence of the crosslinking induced by the metal ion [12, 68, 71]. However, the presence of metal ions produces a lower thermal stability of the complex, as a result of the weakening in the chemical bonds after the coordination of the metal ion that produced changes in the electron density [10, 66]. For example, the T_g value obtained for the polyelectrolyte hydrogel *poly*(EGDE-DA) (**Scheme 2**) was 120.0°C, while that for the Cu(II) hydrogel complex containing 131 mg of Cu(II) per gram of polymer was 169.5 °C. This shift to higher temperature values was due to the stabilization of the *d*-electron of the copper ion on coordination, as expected, and it was also another fact of the crosslink between the polymer chains and the copper ion. For the Co(II) hydrogel complex, the T_g value was 134.1 °C, and it was lower than in the case of copper, in concordance with the low amount of cobalt ions adsorbed to the polymer material (23 mg of Co(II) per gram of polymer), reducing the crosslinking between the polymer chains and cobalt ions [12].

Finally, the polymeric particles loaded with cations were cut into slices to see if these compounds had access to the entire network or were only attached to the surface. In all the cases, they reached the interior binding sites of these particles, and it was impossible to distinguish a core from the exposed surface. These results, together with the swelling properties of these materials, confirm the fact that they are hydrogels. The water molecules and solutes have access to the bulk of the swelled particles. The materials absorb water and dissolved ions. This was demonstrated by the fact that "water adsorption surface" determined for *poly*(EGDE-MAA-2MI) and its copper complex was 287 and 346 $m^2\ g^{-1}$, respectively, clearly indicating the absorption of water molecules [12, 16].

5. Environmental application of hydrogels and metal ion hydrogel complexes

Both natural and synthetic polymeric materials can be used to remove organic and inorganic pollutants given their high load capacities associated with the functional groups present in their chemical structures. Adsorption is the easiest method to remove substances from effluents, but a second residue is generated because pollutants are adsorbed to the material used. Specifically, hydrogels can be used to concentrate different kinds of industrial dyes. Regarding inorganic contaminants adsorbed in different materials, heavy metal ions can be desorbed under acidic conditions from the matrix where they are retained. In these conditions, the metal ions are concentrated, which allows their recovery. Some of the materials that can be used for metal ion uptake have been described throughout this chapter.

On the contrary, organic pollutants can be adsorbed in the first instance, and then oxidative methods where ROS are generated from H_2O_2 can achieve the partial or complete mineralization to CO_2 and H_2O. These catalytic systems are usually called advanced oxidative technologies for wastewater treatment, and some of them will be covered in this section.

Hydrogen peroxide (H_2O_2) is a powerful oxidant used in the degradation of pollutants combined with catalysts and/or UV light to give rise to reactive species such as hydroxyl radical. With respect to the oxidation of aromatic hydrocarbons, Fenton-like reactions (Fe(III)/H_2O_2) are widely used but are only effective in acidic conditions [72]. In contrast, Cu(II)/H_2O_2 systems can be used for similar purposes but in a broader pH range. In turn, the catalytic

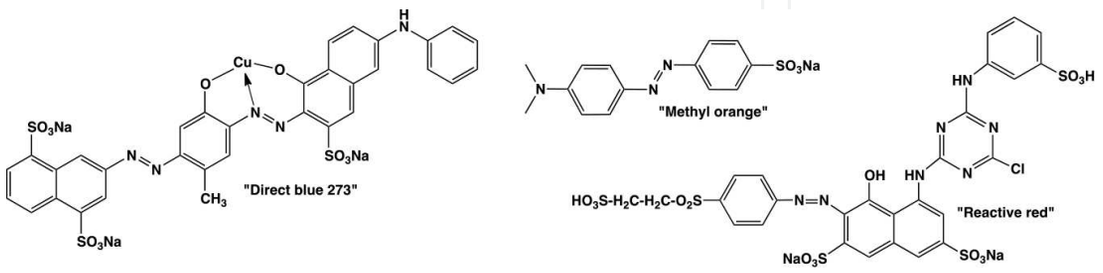

Scheme 7. Chemical structures of some dyes used in the textile industry.

http://dx.doi.org/10.5772/62902

activity of the copper ion in the activation of H_2O_2 with concomitant generation of hydroxyl radicals is enhanced after coordination with pyridine, organic acids, and other chelating agents, but the recovery of these complexes is expensive because they are soluble in water. For these reasons, heterogeneous catalysts are an attractive alternative for decolorization, combining effectiveness, ease of recovery, and reuse potential. Also, transition metals supported on alumina and silica have proved to be more efficient for the activation of H_2O_2 than homogenous catalysts. In addition, complexes of Cu(II) with alumina or chitosan have been used to remove color from industrial waste [73, 74], Cu(II) complexes immobilized on silica particles have been used as catalysts in the hydroxylation of phenols from H_2O_2 [75] and non-soluble Cu(II) chitosan/H_2O_2 systems have been used to degrade anthraquinone and azo dye compounds commonly found in the textile industry [76]. Textile dyes are considered the most common industrial pollutants in waters. In addition, modern dyes are stable to the ineffective conventional treatment methods performed on wastewater (**Scheme 7**). This results in an intensely colored discharge that is released from the factory with a direct negative impact on the environment. Both Cu(II) chitosan and any other modified chitosan coordinated with copper ions can act as efficient heterogeneous catalysts for the activation of H_2O_2, in which radical species (mainly hydroxyl radicals, OH•) are generated, and dyes and other organic pollutants are concomitantly degraded to CO_2 and H_2O. This process is highly dependent on the efficiency in the oxidative capacity of the catalyst, susceptibility of the pollutant, and the amount of H_2O_2 added [76].

However, even when these systems are very effective, some precautions must be taken into account to ensure the catalytic activity. To not affect the structure of the catalyst, the initial concentration of H_2O_2 ($[H_2O_2]_o$) needs to be controlled. As an example, synthetic Cu(II) *poly*(EGDE-MAA-IM or 2MI) hydrogels are stable up to a $[H_2O_2]_o$ = 50 mM since higher concentrations affect the structure of the catalyst (**Scheme 2**) [14, 15]. In addition, at higher $[H_2O_2]_o$, the H_2O_2 molecules combine with OH• radical species to generate superoxide radicals ($O_2^{\bullet -}$) with lower oxidation potential. Moreover, the use of high concentrations of H_2O_2 produces its self-decomposition to O_2 and H_2O [15].

There are some experimental techniques that can be done to do an exhaustive characterization of each Cu(II)-supported material or any other metal complex. Once the coordination behavior and the amount and distribution of the metal ion have been studied, the activation of H_2O_2 can be explored. However, it is also useful to explore the stability of the metal complexes in the experimental conditions in which the catalyst will be used (pH, ionic strength, temperature, etc.).

The reaction with 4-aminoantipyrine is usually used for the detection of free radical species and can be tested in different samples as an easy screening [15, 77]. Nevertheless, it is not able to discern which free radical species are generated through the activation process of H_2O_2 on the catalytic surface. For the correct identification of the radical species generated in diverse Cu(II) complex/H_2O_2 systems, EPR measurements should be made with a spin trap molecule. In this way, a stable radical is formed from the incubation of 5,5-dimethyl-1-pyrroline *N*-oxide (DMPO) solution with a sample obtained from the reaction mixture (Cu-hydrogel/H_2O_2) where the radical (R•) species are generated, thus allowing its detection and identification

through EPR spectroscopy. The EPR spectra obtained depend on the R• nature in the medium since the spectral lines characterize each DMPO-R adduct. As an example, **Figure 4** shows the EPR spectrum obtained by the reaction of DMPO (1 M) with an aliquot from the supernatant of a mixture reaction containing 10 mg of Cu(II) *poly*(EGDE-MAA-IM) hydrogel (q_m Cu(II): 60 mg g^{-1}), $[H_2O_2]_o$ = 25 mM and a final volume of phosphate buffer of 10 mL (pH = 7.0).

The Co(II)-*poly*(EGDE-DA)/H_2O_2 heterogeneous system also produced free radicals that diffused to the solution and were detected by spin trapping experiments with DMPO ($[H_2O_2]_o$ = 63 mM) (**Figure 4E**). The simulation and fits of the experimental spectrum allowed establishing the presence of two species: DMPO-OOH (93%) and DMPO-OH (7%) adducts from anion superoxide ($O_2^{\bullet-}$) and hydroxyl radical (OH•), respectively [12]. In addition, for the coexistence of both hydroxyl and superoxide radical species in cobalt-complexes, it is possible to add the enzyme superoxide dismutase to only visualize the DMPO-OH adduct and to indirectly evidence the presence of the DMPO-OOH (DMPO + $O_2^{\bullet-}$) adduct in the mixture [12].

It is important to note, that, in some cases, ROS can oxidize DMPO and/or the organic matrix, giving rise to nitroxide-like radical and/or carbon-centered radical, respectively, with a characteristic DMPO adduct depending on the reactivity of the system [15].

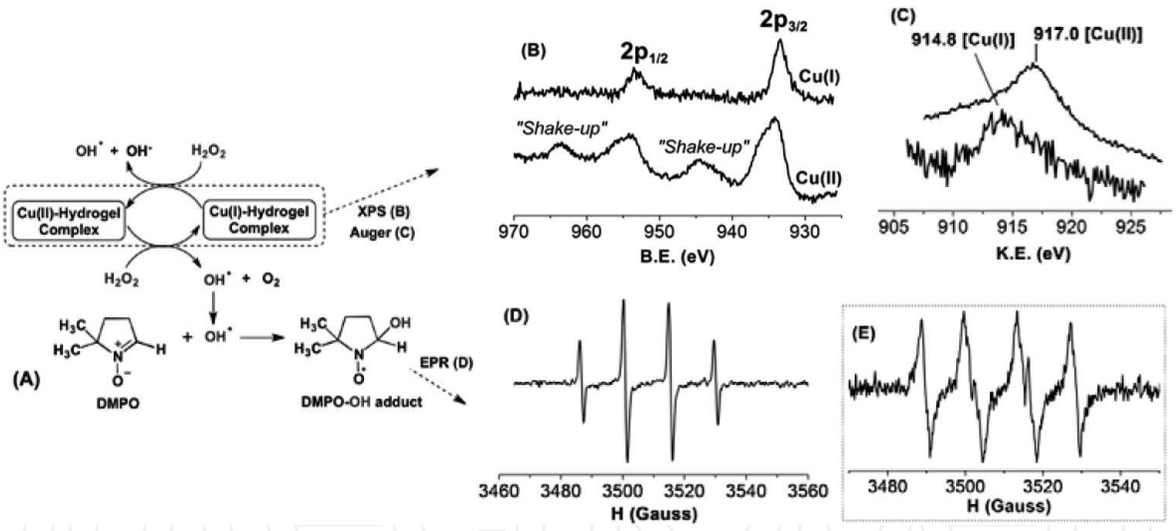

Figure 4. Schematic representation of the inner sphere mechanism where the OH• radicals are generated due to the interconversion between Cu(II)⇔Cu(I) in a Cu(II)- *poly*(EGDE-MAA-IM) hydrogel as a heterogeneous catalyst (A), Cu *2p* region of the XPS spectra (B), Auger spectra for Cu(I) or Cu(II)-hydrogel complexes (C), and the corresponding X-band EPR spectrum of a DMPO-OH adduct obtained from a mixture reaction as indicated (D) [14, 15]. X-band EPR spectra of DMPO-OOH and DMPO-OH adducts obtained from a Co(II)-*poly*(EGDE-DA)/H_2O_2 heterogeneous system as indicated (E) [12]. EPR measurements were performed at X-band on a Bruker EMX plus spectrometer. XPS spectra were collected using a physical electronics PHI 5700 spectrometer.

Then, when the generation of free radical species is identified, it is possible to access to the catalytic system which can describe the mechanism involved in the generation of these species. Particularly, the Cu(II) complexes have been extensively studied, and the most acceptable catalytic cycle involves the reduction of Cu(II) to Cu(I) induced by the action of the H_2O_2, which

http://dx.doi.org/10.5772/62902

is converted to OH• radical (inner sphere mechanism, **Figure 4**). In this aspect, the XPS technique is a valuable tool to analyze changes in the oxidation state of metal centers. For example, the synthetic Cu(II) *poly*(EGDE-MAA-IM) hydrogel system, containing 63 mg of Cu(II) per gram of polymer (**Scheme 2**), after being in contact with a $[H_2O_2]_o$ = 25 mM for 1 hour, produces the reduction of Cu(II) to Cu(I), which can be visualized because the conversion of Cu(I) to Cu(II) is low with the decrease in the consumption of H_2O_2. The Cu *2p* region in the XPS spectrum is different after the treatment with H_2O_2 because characteristic shake-up satellite structures of Cu(II) are not observed. However, the Auger line for copper has to be measured with a short irradiation time due to a photoreduction of Cu(II) to Cu(I). With the correct acquisition of the Auger line for copper, it is possible to prove the presence of Cu(I) species generated by the action of H_2O_2 in a Cu(II) hydrogel system (**Figure 4**) [14]. Furthermore, it has been observed that the ultrahigh vacuum in which the sample is exposed prior to the XPS measurement can produce the reduction of Cu(II) to Cu(I) in Cu(II) *poly*(ethylenimine) complexes [41].

In addition, the catalytic performance of the catalyst can be studied with the azo dye methyl orange as a model compound because its absorbance can be easily monitored as a function of time through UV-visible spectroscopy at 465 nm (**Scheme 7**). In general, the concentration of methyl orange in the solution where the catalyst and H_2O_2 are also present decreases as a consequence of two parallel processes: surface adsorption on the catalyst and oxidative degradation, both following pseudo first-order kinetics [5, 7, 12, 14, 15].

Regarding other metal ion complexes, cobalt complexes can be very useful for soft oxidative procedures in organic chemistry. There are only a few reports related to Co(II) complexes supported in non-soluble polymeric structures, although a Co(II)-crosslinked polyacrylamide can be mentioned as a selective catalyst for the oxidation of olefins and alkyl halides with H_2O_2 in aqueous media [78]. The difference with copper complexes is that the metal ion is converted to Co(III) from the corresponding Co(II) in the presence of H_2O_2 [12, 13, 78].

Regarding environmental applications, our research group observed that the Co(II) *poly*(EGDE-DA) hydrogel/H_2O_2 system is not as reactive for the degradation of methyl orange as the corresponding Cu(II) system supported in the same polymeric structure (**Scheme 2**). It is important to remark that the maximum loading capacities for Co(II) and Cu(II) ions are estimated in 15 and 151 mg g^{-1}. However, although a Co(II) hydrogel/H_2O_2 system can achieve 87% of oxidation of methyl orange in 110 minutes, the Cu(II) hydrogel/H_2O_2 system can do so in 10 minutes. Even when the amount of Co(II) ions is low, the catalytic importance makes this kind of system of interest since the Co(II) can produce superoxide radicals with a lower oxidative potential [12, 13].

6. Remarks

The coordination of a polymeric ligand by a transition metal ion is an efficient way to obtain processable materials with unique and valuable properties. Polymer networks offer new possibilities to scientists for the creation of artificial materials. In recent years, hydrogels with

chelating ligands have attracted the attention of industrial applications. In particular, polyelectrolyte and polyampholyte hydrogels have become of great interest in the macromolecular chemistry area due to their versatility as excellent adsorbents of chemical compounds. Stimulus-sensitive hydrogels are used in a variety of novel applications, including controlled drug delivery, immobilized enzyme systems, separation processes, fuel cells, and sensor development.

The development of polymers containing nitrogen remains a growing area because of their applications in the destabilization of negative colloids in effluents and water clarification, electrophoretic depositions, recovery of heavy metal ions or exchange resins for ions, and the mimicking of active sites of enzymes.

Currently, the main goals for the material science community are the design and synthesis of new hydrogels containing ligand for the uptake of heavy metal ions to reduce the direct impact of this industrial waste on the environment. The characterization of the different non-soluble polymeric structures is limited to the spectroscopic techniques in the solid state, being ss-NMR the principal characterization tool for bulk analysis. However, some sensitivity problems can be resolved with new polarization techniques such as DNP-NMR. In addition, some other surface characterization techniques such as X-ray photoelectron spectroscopy can be used. However, the results provide only information limited to the interface area and not from the bulk content. Particularly, the activation of H_2O_2 from the corresponding Cu(II) and Co(II) hydrogels, obtained from the uptake of Cu(II) or Co(II) ions, can be successfully used with H_2O_2 for the degradation of azo dyes, to reduce the impact of both inorganic or organic pollutants.

Author details

Viviana Campo Dall' Orto and Juan Manuel Lázaro-Martínez*

*Address all correspondence to: lazarojm@ffyb.uba.ar

Universidad de Buenos Aires, Facultad de Farmacia y Bioquímica & IQUIFIB-CONICET, Junín 956 (1113), Ciudad Autónoma de Buenos Aires, Argentina

References

[1] Vijayaraghavan K, Jegan J, Palanivelu K, Velan M. Batch and column removal of copper from aqueous solution using a brown marine alga Turbinaria ornata. Chem Eng J. 2005;106(2):177–84.

[2] Bailey SE, Olin TJ, Bricka RM, Adrian DD. A review of potentially low-cost sorbents for heavy metals. Water Res. 1999;33(11):2469–79.

[3] Kudaibergenov SE. Polyampholytes: Synthesis, Characterization and Application. Springer US; 2002.

[4] Lowe AB, McCormick CL. Synthesis and solution properties of zwitterionic polymers. Chem Rev. 2002;102(11):4177–89.

[5] Janus M, Morawski A. New method of improving photocatalytic activity of commercial Degussa P25 for azo dyes decomposition. Appl Catal B Environ. 2007;75(1–2):118–23.

[6] Lin T, Wu C. Activation of hydrogen peroxide in copper(II)/amino acid/H2O2 systems: Effects of pH and copper speciation. J Catal. 2005;232:117–26.

[7] Shah V, Verma P, Stopka P, Gabriel J, Baldrian P, Nerud F. Decolorization of dyes with copper(II)/organic acid/hydrogen peroxide systems. Appl Catal B Environ. 2003;46(2): 287–92.

[8] Meng X, Zhu J, Yan J, Xie J, Kou X, Kuang X, et al. Studies on the oxidation of phenols catalyzed by a copper(II)-Schiff base complex in aqueous solution under mild conditions. J Chem Technol Biotechnol. 2006;81:2–7.

[9] Bekturov EA, Kudaibergenov SE, Sigitov VB. Complexation of amphoteric copolymer of 2-methyl-5-vinylpyridine-acrylic acid with copper (ll) ions and catalase-like activity of polyampholyte-metal complexes. Polymer (Guildf). 1986;27:1269–72.

[10] Lázaro-Martínez JM, Monti GA, Chattah AK. Insights into the coordination sphere of copper ion in polymers containing carboxylic acid and azole groups. Polymer (Guildf). 2013;54(19):5214–21.

[11] Solomon EI, Sundaram UM, Machonkin TE. Multicopper oxidases and oxygenases. Chem Rev. 1996;96(7):2563–606.

[12] Lombardo Lupano LV, Lázaro Martínez JM, Piehl LL, Rubín de Celis E, Torres Sánchez RM, Campo Dall' Orto V. Synthesis, characterization, and catalytic properties of cationic hydrogels containing copper(II) and cobalt(II) ions. Langmuir. 2014;30(10): 2903–13.

[13] Lombardo Lupano LV, Lázaro Martínez JM, Piehl LL, Rubin de Celis E, Campo Dall' Orto V. Activation of H2O2 and superoxide production using a novel cobalt complex based on a polyampholyte. Appl Catal A Gen. 2013;467:342–54.

[14] Lázaro Martínez JM, Rodríguez-Castellón E, Sánchez RMT, Denaday LR, Buldain GY, Campo Dall' Orto V. XPS studies on the Cu(I,II)–polyampholyte heterogeneous catalyst: An insight into its structure and mechanism. J Mol Catal A Chem. 2011;339(1–2):43–51.

[15] Lázaro Martínez JM, Leal Denis MF, Piehl LL, de Celis ER, Buldain GY, Campo Dall' Orto V. Studies on the activation of hydrogen peroxide for color removal in the presence

of a new Cu(II)-polyampholyte heterogeneous catalyst. Appl Catal B Environ. 2008;82(3–4):273–83.

[16] Lázaro Martínez JM, Chattah AK, Torres Sánchez RM, Buldain GY, Campo Dall' Orto V. Synthesis and characterization of novel polyampholyte and polyelectrolyte polymers containing imidazole, triazole or pyrazole. Polymer (Guildf). 2012;53(6): 1288–97.

[17] Alfrey T, Morawetz H. Amphoteric polyelectrolytes. I. 2-Vinylpyridine—methacrylic acid copolymers. J Am Chem Soc. 1952;74(2):436–8.

[18] Annenkov VV, Danilovtseva EN, Tenhu H, Aseyev V, Hirvonen SP, Mikhaleva AI. Copolymers of 1-vinylimidazole and (meth)acrylic acid: Synthesis and polyelectrolyte properties. Eur Polym J. 2004;40(6):1027–32.

[19] Leal Denis MF, Carballo RR, Spiaggi AJ, Dabas PC, Campo Dall' Orto V, Martínez JML, et al. Synthesis and sorption properties of a polyampholyte. React Funct Polym. 2008;68(1):169–81.

[20] Krasia TC, Patrickios CS. Synthesis and aqueous solution characterization of amphiphilic diblock copolymers containing carbazole. Polymer (Guildf). 2002;43(10):2917–20.

[21] Kumar A, Lahiri SS, Singh H. Development of PEGDMA: MAA based hydrogel microparticles for oral insulin delivery. Int J Pharm. 2006;323(1–2):117–24.

[22] Jang J, Ishida H. A study of corrosion protection on copper by new polymeric agents: Silane-modified imidazoles. Corros Sci. 1992;33(7):1053–66.

[23] Jilge G, Sébille B, Vidal-Madjar C, Lemque R, Unger KK. Optimisation of fast protein separations on non-porous silica-based strong anion exchangers. Chromatographia. 1993;37(11):603–7.

[24] Kowalik-Jankowska T, Ruta-Dolejsz M, Wiśniewska K, Łankiewicz L, Kozłowski H. Copper(II) complexation by human and mouse fragments (11–16) of β-amyloid peptide. J Chem Soc, Dalton Trans. 2000:4511–9.

[25] Casolaro M, Ito Y, Ishii T, Bottari S, Samperi F, Mendichi R. Stimuli-responsive poly(ampholyte)s containing L-histidine residues: Synthesis and protonation thermodynamics of methacrylic polymers in the free and in the cross-linked gel forms. Express Polym Lett. 2008;2(3):165–83.

[26] Casolaro M, Bottari S, Cappelli A, Mendichi R, Ito Y. Vinyl polymers based on l-histidine residues. Part 1. The thermodynamics of poly(ampholyte)s in the free and in the cross-linked gel form. Biomacromolecules. 2004;5(4):1325–32.

[27] Barton JM, Hamerton I, Howlin BJ, Jones JR, Liu S. Studies of cure schedule and final property relationships of a commercial epoxy resin using modified imidazole curing agents. Polymer (Guildf). 1998;39(10):1929–37.

[28] Kwok AY, Qiao GG, Solomon DH. Interpenetrating amphiphilic polymer networks of poly(2-hydroxyethyl methacrylate) and poly(ethylene oxide). Chem Mater. 2004;16(26):5650–8.

[29] van Berkel PM, Driessen WL, Reedijk J, Sherrington DC, Zitsmanis A. Metal-ion binding affinity of azole-modified oxirane and thiirane resins. React Funct Polym. 1995;27(1):15–28.

[30] van Berkel PM, Punt M, Koolhaas GJAA, Driessen WL, Reedijk J, Sherrington DC. Highly copper(II)-selective chelating ion-exchange resins based ion bis(imidazole)-modified glycidyl methacrylate copolymers. React Funct Polym. 1997;32(2):139–51.

[31] Wan Ngah WS, Endud CS, Mayanar R. Removal of copper(II) ions from aqueous solution onto chitosan and cross-linked chitosan beads. React Funct Polym. 2002;50(2): 181–90.

[32] Nada AAM, Alkady MY, Fekry HM. Synthesis and characterization of grafted cellulose for use in water and metal ions sorption. BioResources. 2008;3:46–59.

[33] Blanc F, Copéret C, Lesage A, Emsley L. High resolution solid state NMR spectroscopy in surface organometallic chemistry: Access to molecular understanding of active sites of well-defined heterogeneous catalysts. Chem Soc Rev. 2008;37:518–26.

[34] Harris RK. Nuclear Magnetic Resonance Spectroscopy: A Physiocochemical View. London: Logman Scientific and Technical; 1986.

[35] Lowe IJ. Free induction decays of rotating solids. Phys Rev Lett. 1959;2(7):285–7.

[36] Andrew ER, Bradbury A, Eades RG. Removal of dipolar broadening of nuclear magnetic resonance spectra of solids by specimen rotation. Nature. 1959;183(4678): 1802–3.

[37] Hartmann SR, Hahn EL. Nuclear double resonance in the rotating frame. Phys Rev. 1962;128(5):2042–53.

[38] Fung BM, Khitrina K, Ermolaev K. An improved broadband decoupling sequence for liquid crystals and solids. J Magn Reson. 2000;142(1):97–101.

[39] Lombardo Lupano LV, Lázaro-Martínez JM, Vizioli NM, Torres DI, Campo V, Orto D, et al. Synthesis of water-soluble oligomers from imidazole, ethyleneglycol diglycidyl ether, and methacrylic acid. An insight into the chemical structure, aggregation behavior and formation of hollow spheres. Macromol Mater Eng. 2016;301(2):167–81.

[40] Wu XL, Zilm KW. Complete spectral editing in CPMAS NMR. J Magn Reson Ser A. 1993;102(2):205–13.

[41] Lázaro-Martínez JM, Rodríguez-Castellón E, Vega D, Monti GA, Chattah AK. Solid-state studies of the crystalline/amorphous character in linear poly(ethylenimine hydrochloride) (PEI·HCl) polymers and their copper complexes. Macromolecules. 2015;48(4):1115–25.

[42] Power WP. High resolution magic angle spinning – applications to solid phase synthetic systems and other semi-solids. Annu Reports NMR Spectrosc. 2003;51(03): 261–95.

[43] Higashi K, Yamamoto K, Pandey MK, Mroue KH, Moribe K, Yamamoto K, et al. Insights into atomic-level interaction between mefenamic acid and Eudragit EPO in a supersaturated solution by high-resolution magic-angle spinning NMR spectroscopy. Mol Pharm. 2014;11(1):351–7.

[44] Maly T, Debelouchina GT, Bajaj VS, Hu K, Joo C, Mak-Jurkauskas ML, et al. Dynamic nuclear polarization at high magnetic fields. J Chem Phys. 2008;128(5):052211.

[45] Lesage A, Lelli M, Gajan D, Caporini MA, Vitzthum V, Miéville P, et al. Surface enhanced NMR spectroscopy by dynamic nuclear polarization. J Am Chem Soc. 2010;132(44):15459–61.

[46] Zagdoun A, Casano G, Ouari O, Lapadula G, Rossini AJ, Lelli M, et al. A slowly relaxing rigid biradical for efficient dynamic nuclear polarization surface-enhanced NMR spectroscopy: Expeditious characterization of functional group manipulation in hybrid materials. J Am Chem Soc. 2012;134(4):2284–91.

[47] Wagner CD, Riggs WM, Davis LE, Moulder JF, Muilenberg GE. Handbook of X-ray photoelectron spectroscopy. In Muilenberg GE, editor. Minnesota: Perkin-Elmer Corporation; 1979.

[48] Brunauer S, Emmett PH, Teller E. Adsorption of gases in multimolecular layers. J Am Chem Soc. 1938;60(1):309–19.

[49] Langmuir I. The adsorption of gases on plane surfaces of glass, mica and platinum. J Am Chem Soc. 1918;40(9):1361–403.

[50] Do DD. Adsorption analysis: Equilibria and kinetics, Vol. 2. London: Imperial College Press; 1998.

[51] Aharoni C, Sparks DL. Rates of Soil Chemical Processes. In Sparks DL and Suarez DL, editors. Madison, WI; Soil Science Society of America 1991. 1–18 p.

[52] Hsieh C-T, Teng H. Langmuir and Dubinin–Radushkevich analyses on equilibrium adsorption of activated carbon fabrics in aqueous solutions. J Chem Technol Biotechnol. 2000;75(11):1066–72.

[53] Hobson JP. Physical adsorption isotherms extending from ultrahigh vacuum to vapor pressure. J Phys Chem. 1969;73(8):2720–7.

[54] Gübbük IH, Güp R, Ersöz M. Synthesis, characterization, and sorption properties of silica gel-immobilized Schiff base derivative. J Colloid Interface Sci. 2008;320:376–82.

[55] Hadi M, Samarghandi MR, McKay G. Equilibrium two-parameter isotherms of acid dyes sorption by activated carbons: Study of residual errors. Chem Eng J. 2010;160(2): 408–16.

[56] Burnham KP, Anderson DR, Huyvaert KP. AIC model selection and multimodel inference in behavioral ecology: Some background, observations, and comparisons. Behav Ecol Sociobiol. 2011;65(1):23–35.

[57] Cheung C, Porter J, Mckay G. Sorption kinetic analysis for the removal of cadmium ions from effluents using bone char. Water Res. 2001;35(3):605–12.

[58] Pérez-Marín AB, Zapata VM, Ortuño JF, Aguilar M, Sáez J, Lloréns M. Removal of cadmium from aqueous solutions by adsorption onto orange waste. J Hazard Mater. 2007;139(1):122–31.

[59] Ho Y. The kinetics of sorption of divalent metal ions onto sphagnum moss peat. Water Res. 2000;34(3):735–42.

[60] Loukidou MX, Zouboulis AI, Karapantsios TD, Matis KA. Equilibrium and kinetic modeling of chromium(VI) biosorption by Aeromonas caviae. Colloids Surfaces A Physicochem Eng Asp. 2004;242(1–3):93–104.

[61] Copello GJ, Diaz LE, Campo Dall' Orto V. Adsorption of Cd(II) and Pb(II) onto a one step-synthesized polyampholyte: Kinetics and equilibrium studies. J Hazard Mater. 2012;217–218:374–81.

[62] Teng H, Hsieh C-T. Activation energy for oxygen chemisorption on carbon at low temperatures. Ind Eng Chem Res. 1999;38(1):292–7.

[63] Kuo S, Lotse EG. Kinetics of phosphate adsorption and desorption by hematite and gibbsite. Soil Sci. 1973;116(6):400–406.

[64] Bache BW, Williams EG. A phosphate sorption index for soils. J Soil Sci. 1971;22(3):289–301.

[65] Ho Y., McKay G. Pseudo-second order model for sorption processes. Process Biochem. 1999;34(5):451–65.

[66] Lázaro Martínez JM, Chattah AK, Monti GA, Leal Denis MF, Buldain GY, Campo Dall' Orto V. New copper(II) complexes of polyampholyte and polyelectrolyte polymers: Solid-state NMR, FTIR, XRPD and thermal analyses. Polymer (Guildf). 2008;49(25):5482–9.

[67] Peisach J, Blumberg WE. Structural implications derived from the analysis of electron paramagnetic resonance spectra of natural and artificial copper proteins. Arch Biochem Biophys. 1974;165(2):691–708.

[68] Andersson M, Hansson Ö, Öhrström L, Idström A, Nydén M. Vinylimidazole copolymers: Coordination chemistry, solubility, and cross-linking as function of Cu2+ and Zn2+ complexation. Colloid Polym Sci. 2011;289(12):1361–72.

[69] Sun Z, Jin L, Zhang S, Shi W, Pu M, Wei M, et al. An optical sensor based on H-acid/layered double hydroxide composite film for the selective detection of mercury ion. Anal Chim Acta. 2011;702(1):95–101.

[70] Fang X, Chen R, Xiao L, Chen Q. Synthesis and characterization of Sm(III)–hyperbranched poly(ester-amide) complex. Polym Int. 2011;60(1):136–40.

[71] Belfiore LA, Graham H, Uedat E. Ligand field stabilization in nickel complexes that exhibit extraordinary glass transition temperature enhancement. Macromolecules. 1992;25:2935–9.

[72] Kang N, Lee DS, Yoon J. Kinetic modeling of Fenton oxidation of phenol and monochlorophenols. Chemosphere. 2002;47(9):915–24.

[73] Gemeay AH, Salem MA, Salem IA. Activity of silica-alumina surface modified with some transition metal ions. Colloids Surfaces A Physicochem Eng Asp. 1996;117:245–52.

[74] Salem IA. Kinetics of the oxidative color removal and degradation of bromophenol blue with hydrogen peroxide catalyzed by copper(II)-supported alumina and zirconia. Appl Catal B Environ. 2000;28(3–4):153–62.

[75] Ray S, Mapolie SF, Darkwa J. Catalytic hydroxylation of phenol using immobilized late transition metal salicylaldimine complexes. J Mol Catal A Chem. 2007;267(1–2):143–8.

[76] Šuláková R, Hrdina R, Soares GMB. Oxidation of azo textile soluble dyes with hydrogen peroxide in the presence of Cu(II)–chitosan heterogeneous catalysts. Dye Pigment. 2007;73(1):19–24.

[77] Ettinger M, Ruchhoft C, Lishka R. Sensitive 4-aminoantipyrine method for phenolic compounds. Anal Chem. 1951;23(12):1783–8.

[78] Tamami B, Ghasemi S. Modified crosslinked polyacrylamide anchored Schiff base–cobalt complex: A novel nano-sized heterogeneous catalyst for selective oxidation of olefins and alkyl halides with hydrogen peroxide in aqueous media. Appl Catal A Gen. 2011;393(1–2):242–50.